Dana Kotorová

Comparison of the 3D Numerical Schemes for Solving Curvature Driven Level Set Equation Based on Discrete Duality Finite Volumes

Acta Universitatis Palackianae Olomucensis. Facultas Rerum Naturalium. Mathematica, Vol. 53 (2014), No. 2, 71–83

Persistent URL: `http://dml.cz/dmlcz/144040`

Acta Univ. Palacki. Olomuc., Fac. rer. nat.,
Mathematica **53**, 2 (2014) 71–83

Comparison of the 3D Numerical Schemes for Solving Curvature Driven Level Set Equation Based on Discrete Duality Finite Volumes*

Dana KOTOROVÁ

Department of Mathematics and Descriptive Geometry
Faculty of Civil Engineering, Slovak University of Technology Bratislava
Radlinského 11, 813 68 Bratislava, Slovak Republic
e-mail: dana.kotorova@stuba.sk

(Received May 30, 2013)

Abstract

In this work we describe two schemes for solving level set equation in 3D with a method based on finite volumes. These schemes use the so-called dual volumes as in [3, 7], where they are used for the nonlinear elliptic equations. We describe these schemes theoretically and also compare results of the numerical experiments based on exact solution using proposed schemes.

Key words: Mean curvature flow, level set equation, numerical solution, semi-implicit scheme, discrete duality finite volume method (DDFV).

2010 Mathematics Subject Classification: 35K20, 35K55, 65M08

1 Introduction

The level set equation (1) can be used in many different applications—motion of interfaces, in thermomechanics, computational fluid dynamics, smoothing and segmentation of images.

The unknown function $u(t,x)$ in

$$u_t - |\nabla u|\nabla.\left(\frac{\nabla u}{|\nabla u|}\right) = 0, \tag{1}$$

*Supported by APVV-0184-10 and VEGA 1/1137/12.

is defined in $Q_T = I \times \Omega$, $\Omega \subset \mathbb{R}^3$ is a bounded Lipschitz domain, $I = [0, T]$, $T > 0$ is a time interval. We will consider the equation accompanied with the zero Neumann boundary conditions and by an initial condition:

$$\partial_\nu u = 0 \quad \text{on } I \times \partial\Omega, \tag{2}$$

$$u(0, x) = u^0(x). \tag{3}$$

2 DDFV schemes in 3D

In this paper we will consider Ω as a prism $\Omega = \langle a_1, b_1 \rangle \times \langle a_2, b_2 \rangle \times \langle a_3, b_3 \rangle$. Let us describe creating of the mesh. We will divide each edge in the following way: $x_0 = a_1$, $x_i = a_1 + i \cdot h$, $i = 1, \ldots, N_1$; $y_0 = a_2$, $y_i = a_2 + i \cdot h$, $i = 1, \ldots, N_2$; $z_0 = a_3$, $z_i = a_3 + i \cdot h$, $i = 1, \ldots, N_3$. We can denote then x_{ijk} as the center of the original finite volume V_{ijk}.

The numerical schemes we will describe in this work are based on the dual finite volumes. Hermeline and also Coudiére with Hubert used these methods for the elliptic partial differential equations. Their schemes were inspiring for us and in this work we will use both of these schemes for the nonlinear parabolic PDE. For the better orientation we will name our schemes after the above mentioned authors.

The basic construction of the numerical scheme will be similar in both cases. We will choose a uniform discrete time step $\tau = \frac{T}{N}$ and replace the time derivative in (1) by the backward difference as in [6]. If we denote the approximated solution at time $n \cdot \tau$ by u^n, we will get

$$\frac{1}{|\nabla u^{n-1}|} \frac{u^n - u^{n-1}}{\tau} = \nabla . \left(\frac{\nabla u^n}{|\nabla u^{n-1}|} \right). \tag{4}$$

Both presented schemes differ in a space discretization and computation of the gradient.

We will divide our domain into finite volumes and let us denote one of them by V. The edges (in our case is by edge understood the square face) of this finite volume will be denoted by e. As it is typical in the finite volume methodology (see [5]), we will integrate (4) over a finite volume V, and using the divergence theorem we get an integral formulation of (4).

$$\int\limits_V \frac{1}{|\nabla u^{n-1}|} \frac{u^n - u^{n-1}}{\tau} dx = \sum_{e \in \partial V} \int\limits_e \frac{1}{|\nabla u^{n-1}|} \frac{\partial u^n}{\partial \nu} ds \tag{5}$$

where ν is a unit outer normal to the boundary of V and e are the edges of the ∂V. Now the exact “fluxes” on the right-hand side and the ”capacity function” $\frac{1}{|\nabla u^{n-1}|}$ on the left-hand side will be approximated numerically.

Because of the gradients in the denominator in this equation, we define, according to the Evans–Spruck regularization [4], Q_e, $Q_e = \sqrt{|\nabla u_e| + \epsilon^2}$, $\epsilon > 0$, as a regularized norm of the gradient on voxel edges Q_e (right-hand side of (5)), and, the regularized averaged gradient inside the finite volume AQ_V (left-hand side of (5)), computed from the solution known from the previous $(n-1)^{\text{st}}$ time step

$$AQ_V = \frac{1}{6} \sum_{e \in \partial V} Q_e$$

For the approximation of the left-hand side of (5) we get

$$\int_V \frac{1}{|\nabla u^{n-1}|} \frac{u^n - u^{n-1}}{\tau} dx \approx \frac{m(V)}{AQ_V} \; \frac{u_V^n - u_V^{n-1}}{\tau}, \tag{6}$$

where $m(V)$ is the measure of a finite volume V and u_V^n is the approximated value in the center of the finite volume V in the time step n. The approximation of the right-hand side, is given by:

$$\sum_{e \in \partial V} \int_e \frac{1}{|\nabla u^{n-1}|} \frac{\partial u^n}{\partial \nu} ds \approx \sum_{e \in \partial V} \frac{m(e)}{Q_e} \; \frac{u_V^n - u_{\overline{V}}^n}{d_{v\overline{v}}}, \tag{7}$$

where u_V and $u_{\overline{V}}$ represent the values in the time step n in the center of the finite volume V and in the center of the neighboring finite volume, respectively, $m(e)$ is the measure of the edge of the finite volume, and $d_{v\overline{v}}$ denotes the distance between two neighboring volume centers.

2.1 "Hermeline" scheme

Now we will describe our understanding of the finite volume mesh in more details. In this scheme we will divide our domain into two meshes. Both meshes will consist of the set of cubes (see Figure 1).

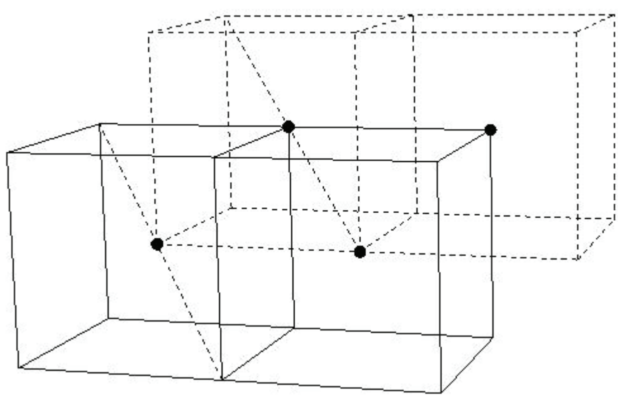

Figure 1: Original (solid lines cubes) and dual (dashed lines cubes) mesh

We restrict our considerations to uniform cubic co-volumes with size length h. Then, e.g.,

$$m(V) = h^3, \quad m(e) = h^2, \quad d_{v\overline{v}} = h.$$

The original volume mesh will consist of the cells $V_{ijk} \in \mathcal{T}_h$. Dual mesh will be shifted to the north-east and will consist of the cells $\overline{V}_{ijk} \in \overline{\mathcal{T}}_h$. Discrete values of the unknown function u_{ijk} will be given in the centers of the original volumes $V_{ijk} \in \mathcal{T}_h$. The dual unknowns v_{ijk} will be given in the centers of the dual volumes. Now we will describe notation for the original volume mesh, for the dual mesh the notation will be the same, but barred and the unknown function will be denoted by v. For each volume $V_{ijk} \in \mathcal{T}_h$, let N_{ijk} represent the set of all neighboring volumes $V_{i+p,j+q,k+r}$, $p, q, r \in \{-1, 0, 1\}$, $|p|+|q|+|r| = 1$. The face of the finite volume will be denoted by e_{ijk}^{pqr}.

We will use the notation for approximated piecewise constant functions $u_h(x) = u_{ijk}$ and $v_h(\overline{x}) = v_{ijk}$, where x_{ijk} and $\overline{x}_{ijk}$ are the centers of the volumes V_{ijk} and $\overline{V}_{ijk}$, respectively. We will also use $u_{h,\tau}(t, x) = u_{ijk}^n$ and $v_{h,\tau}(t, \overline{x}) = v_{ijk}^n$, where $x \in V_{ijk}$, $\overline{x} \in \overline{V}_{ijk}$ and $t \in ((n-1)\tau, n\tau)$ and $u_{h,\tau}(t, x)$ and $v_{h,\tau}(t, \overline{x})$ are the piecewise constant functions in space and time.

To estimate the value of the gradient in (7) on every edge e_{ijk}^{pqr} of the finite volume V_{ijk} we will use the diamond (see Figure 2). The face on which we want to approximate the gradient, will be divided into 2 parts by the diagonal line as in [7, 9] and the gradient will be approximated in both of these parts.

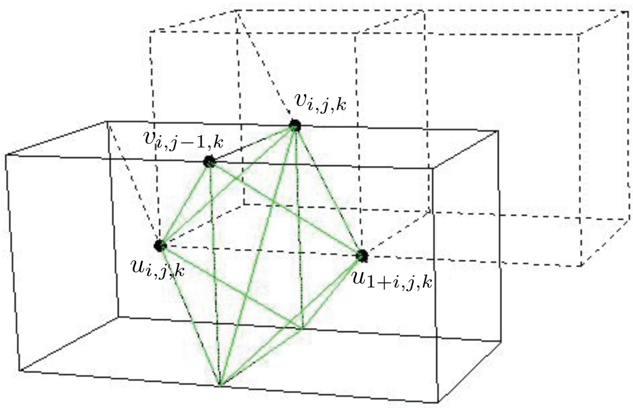

Figure 2: Diamond in the original mesh

The total value of the gradient will be then estimated by

$$|\nabla u_D| = \left| \frac{1}{2}(\nabla u_{D_1} + \nabla u_{D_2}) \right|.$$

For illustration we will show, how the gradient looks like for the right, the back and the top edges of the original volume. How the gradient looks like in general, can be seen in [9].

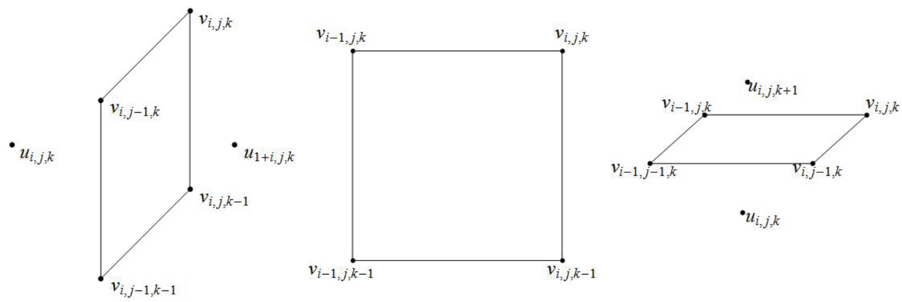

Figure 3: The detail of the right (left), the back (middle) and the top (right) face of the original mesh

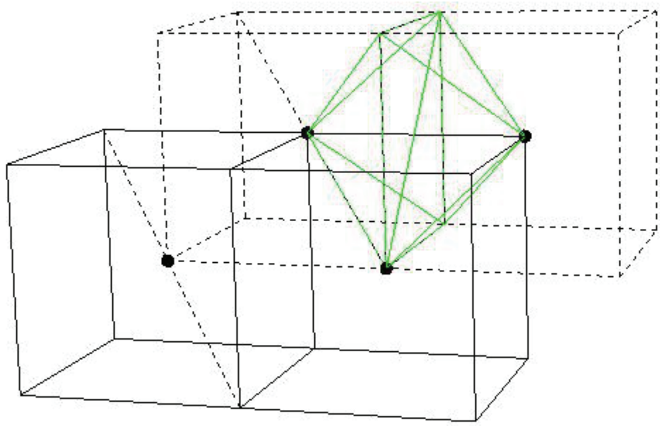

Figure 4: Diamond in the dual mesh

To represent the approximated gradient on the right face, we will use the notation $\nabla^{100} u^n_{ijk}$.

$$\nabla^{100} u^n_{ijk} = \Big(\frac{u^n_{i+1,j,k} - u^n_{ijk}}{h}, \frac{v^n_{ijk} + v^n_{i,j,k-1} - v^n_{i,j-1,k} - v^n_{i,j-1,k-1}}{2h}, \frac{v^n_{i,j-1,k} + v^n_{ijk} - v^n_{i,j-1,k-1} - v^n_{i,j,k-1}}{2h}\Big),$$

For representing the approximated gradient on the back face, we will use the notation $\nabla^{010} u^n_{ijk}$.

$$\nabla^{010} u^n_{ijk} = \Big(\frac{v^n_{i,j,k-1} + v^n_{ijk} - v^n_{i-1,j,k-1} - v^n_{i-1,j,k}}{2h}, \frac{u^n_{i,j+1,k} - u^n_{ijk}}{h}, \frac{v^n_{i-1,j,k} + v^n_{ijk} - v^n_{i-1,j,k-1} - v^n_{i,j,k-1}}{2h}\Big).$$

And for representing the approximated gradient on the top face, we will use the notation $\nabla^{001} u^n_{ijk}$.

$$\nabla^{001} u^n_{ijk} = \Big(\frac{v^n_{ijk} + v^n_{i,j-1,k} - v^n_{i-1,j,k} - v^n_{i-1,j-1,k}}{2h}, \\ \frac{v^n_{i-1,j,k} + v^n_{ijk} - v^n_{i-1,j-1,k} - v^n_{i,j-1,k}}{2h}, \frac{u^n_{i,j,k+1} - u^n_{ijk}}{h} \Big).$$

To approximate the gradient in the dual mesh we will use the same procedure. The gradient will be estimated in the similar way as in the original mesh. The diamond will be understood in the same way as before, but it will be situated in the dual volume (see Figure 4).

The approximated values of the gradient on the particular faces of the dual volume could be again seen in [9].

At the end, after putting together all the above mentioned considerations and using the finite volume procedure described before, we obtain the linear system of equations we have to solve in every discrete time step n, $n = 1, \dots, N$, where N is the total number of time steps.

$$\frac{u^n_{ijk}\ h^3}{\tau\ AQ^{n-1}_{ijk}} + \sum_{|p|+|q|+|r|=1} \frac{\left(u^n_{ijk} - u^n_{i+p,j+q,k+r}\right) h^2}{Q^{pqr;n-1}_{ijk}\ h} = \frac{h^3\ u^{n-1}_{ijk}}{\tau\ AQ^{n-1}_{ijk}}, \tag{8}$$

$$\frac{v^n_{ijk}\ h^3}{\tau\ \overline{AQ}^{n-1}_{ijk}} + \sum_{|p|+|q|+|r|=1} \frac{\left(v^n_{ijk} - v^n_{i+p,j+q,k+r}\right) h^2}{\overline{Q}^{pqr;n-1}_{ijk}\ h} = \frac{h^3\ v^{n-1}_{ijk}}{\tau\ \overline{AQ}^{n-1}_{ijk}}. \tag{9}$$

2.2 "Coudiére–Hubert" scheme

In this case we will consider three meshes. First two meshes will consist of the set of cubes (see Figure 1) as in the previous scheme. The original and dual unknowns will be again given, as before, in the centers of the original and dual volumes and denoted by u and v, respectively.

The third mesh will consist of the face and edge volumes (see Figure 5).

The face unknowns wx, wy and wz will be given in the centers of the right, the back and the top faces of the original finite volume. The edge unknowns zx, zy and zz will be given in the middle of the edges of the original finite volume (as plotted in Figure 7).

We will consider 4 diamonds (see the diamond in Figure 6) on every face of the original finite volume as in [3, 10]. These diamonds will be denoted as D_1, D_2, D_3 and D_4. To define these diamonds on every face of the original finite volume, we will use the following notation.

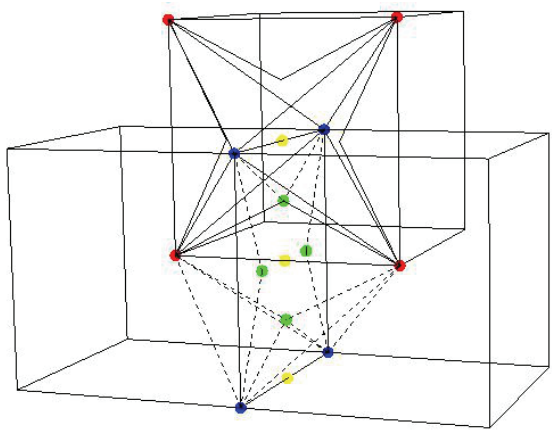

Figure 5: Face volume (dashed lines) and edge volume (solid lines) in the original mesh

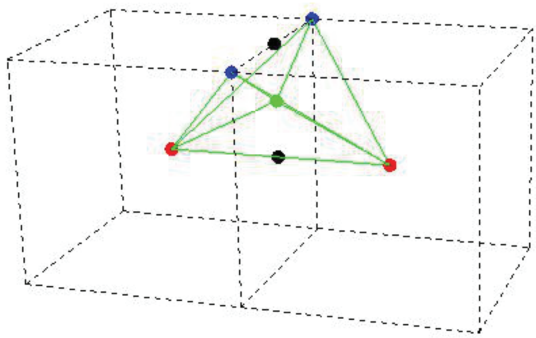

Figure 6: Diamond D1 in the right face of the original volume

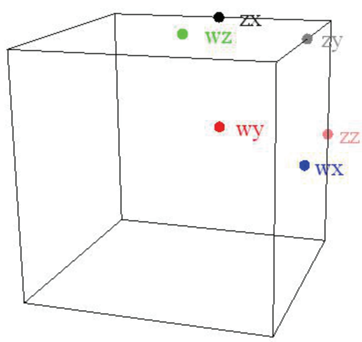

Figure 7: Values of the wx (blue), wy (red), wz (green), zx (black), zy (gray) and zz (pink) variables on the original finite volume

The diamonds on the right face of the original volume V_{ijk} will be denoted as D_1X_{ijk}, D_2X_{ijk}, D_3X_{ijk} and D_4X_{ijk}. The diamonds on the back face of the original volume V_{ijk} will be denoted as D_1Y_{ijk}, D_2Y_{ijk}, D_3Y_{ijk} and D_4Y_{ijk}. The diamonds on the top face of the original volume V_{ijk} will be denoted as D_1Z_{ijk}, D_2Z_{ijk}, D_3Z_{ijk} and D_4Z_{ijk}.

Let us show how the gradients look like on the right, on the back and on the top faces, respectively.

right face:

$$\begin{aligned}
\nabla D_1X_{ijk} &= \left(\frac{u^n_{i+1,j,k}-u^n_{ijk}}{h}, \frac{v^n_{ijk}-v^n_{i,j-1,k}}{h}, \frac{zy^n_{ijk}-wx^n_{ijk}}{\frac{h}{2}}\right)\\
\nabla D_2X_{ijk} &= \left(\frac{u^n_{i+1,j,k}-u^n_{ijk}}{h}, \frac{wx^n_{ijk}-zz^n_{i,j-1,k}}{\frac{h}{2}}, \frac{v^n_{i,j-1,k}-v^n_{i,j-1,k-1}}{h}\right)\\
\nabla D_3X_{ijk} &= \left(\frac{u^n_{i+1,j,k}-u^n_{ijk}}{h}, \frac{v^n_{i,j,k-1}-v^n_{i,j-1,k-1}}{h}, \frac{wx^n_{ijk}-zy^n_{i,j,k-1}}{\frac{h}{2}}\right)\\
\nabla D_4X_{ijk} &= \left(\frac{u^n_{i+1,j,k}-u^n_{ijk}}{h}, \frac{zz^n_{ijk}-wx^n_{ijk}}{\frac{h}{2}}, \frac{v^n_{ijk}-v^n_{i,j,k-1}}{h}\right)
\end{aligned}$$

back face:

$$\begin{aligned}
\nabla D_1Y_{ijk} &= \left(\frac{v^n_{ijk}-v^n_{i-1,j,k}}{h}, \frac{u^n_{i,j+1,k}-u^n_{ijk}}{h}, \frac{zx^n_{ijk}-wy^n_{ijk}}{\frac{h}{2}}\right)\\
\nabla D_2Y_{ijk} &= \left(\frac{wy^n_{ijk}-zz^n_{i-1,j,k}}{\frac{h}{2}}, \frac{u^n_{i,j+1,k}-u^n_{ijk}}{h}, \frac{v^n_{i-1,j,k}-v^n_{i-1,j,k-1}}{h}\right)\\
\nabla D_3Y_{ijk} &= \left(\frac{v^n_{i,j,k-1}-v^n_{i-1,j,k-1}}{h}, \frac{u^n_{i,j+1,k}-u^n_{ijk}}{h}, \frac{wy^n_{ijk}-zx^n_{i,j,k-1}}{\frac{h}{2}}\right)\\
\nabla D_4Y_{ijk} &= \left(\frac{zz^n_{ijk}-wy^n_{ijk}}{\frac{h}{2}}, \frac{u^n_{i,j+1,k}-u^n_{ijk}}{h}, \frac{v^n_{ijk}-v^n_{i,j,k-1}}{h}\right)
\end{aligned}$$

top face:

$$\begin{aligned}
\nabla D_1Z_{ijk} &= \left(\frac{v^n_{ijk}-v^n_{i-1,j,k}}{h}, \frac{zx^n_{ijk}-wz^n_{ijk}}{\frac{h}{2}}, \frac{u^n_{i,j,k+1}-u^n_{ijk}}{h}\right)\\
\nabla D_2Z_{ijk} &= \left(\frac{wz^n_{ijk}-zy^n_{i-1,j,k}}{\frac{h}{2}}, \frac{v^n_{i-1,j,k}-v^n_{i-1,j-1,k}}{h}, \frac{u^n_{i,j,k+1}-u^n_{ijk}}{h}\right)\\
\nabla D_3Z_{ijk} &= \left(\frac{v^n_{i,j-1,k}-v^n_{i-1,j-1,k}}{h}, \frac{wz^n_{ijk}-zx^n_{i,j-1,k}}{\frac{h}{2}}, \frac{u^n_{i,j,k+1}-u^n_{ijk}}{h}\right)\\
\nabla D_4Z_{ijk} &= \left(\frac{zy^n_{ijk}-wz^n_{ijk}}{\frac{h}{2}}, \frac{v^n_{ijk}-v^n_{i,j-1,k}}{h}, \frac{u^n_{i,j,k+1}-u^n_{ijk}}{h}\right)
\end{aligned}$$

To see how the approximated values of the gradients look like at the particular faces and for the particular unknowns, see [10]. Because the original and the dual volumes have the same shape, let us consider $m(V_{ijk}) = m(\overline{V}_{ijk}) = m(V)$ to be the measure of the finite volume and $m(e_{ijk}^{pqr}) = m(\overline{e}_{ijk}^{pqr}) = m(e)$ to be the measure of the faces of the original and dual volumes.

Let us denote by $m(F)$ the measure of the face volume (the green and also the gray volume in Figure 5) and by $m(E)$ the measure of the four edges of the face-edge mesh.

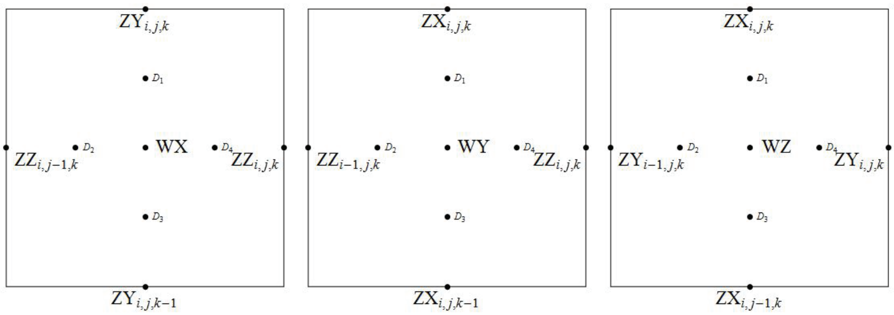

Figure 8: The detail of the right (left), the back (middle) and the top (right) face of the original mesh

The distance between two neighboring volume centers will be denoted as d.

After applying finite volume procedure, we obtain the linear system of the equations we have to solve in every discrete time step n, $n = 1, \ldots, N$, where N is the total number of time steps.

$$\frac{u_{ijk}^{n}\ m(V)}{AQP_{ijk}^{n-1}} + \tau \sum_{|p|+|q|+|r|=1} \frac{(u_{ijk}^{n} - u_{i+p,j+q,k+r}^{n})\ m(e)}{QP_{ijk}^{pqr;n-1}\ d} = \frac{m(V)\ u_{ijk}^{n-1}}{AQP_{ijk}^{n-1}},$$

$$\frac{v_{ijk}^{n}\ m(V)}{AQD_{ijk}^{n-1}} + \tau \sum_{|p|+|q|+|r|=1} \frac{(v_{ijk}^{n} - v_{i+p,j+q,k+r}^{n})\ m(e)}{QD_{ijk}^{pqr;n-1}\ d} = \frac{m(V)\ v_{ijk}^{n-1}}{AQD_{ijk}^{n-1}},$$

$$\frac{(wx_{ijk}^{n} - wx_{ijk}^{n-1})\ m(F)}{\tau\ AQF_{ijk}^{n-1}} + \frac{(wx_{ijk}^{n} - zy_{ijk}^{n})\ m(E)}{QF_{ijk}^{00-1;n-1}\ d} + \frac{(wx_{ijk}^{n} - zz_{i,j-1,k}^{n})\ m(E)}{QF_{ijk}^{0-10;n-1}\ d}$$
$$+ \frac{(wx_{ijk}^{n} - zy_{i,j,k-1}^{n})\ m(E)}{QF_{ijk}^{00-1;n-1}\ d} + \frac{(wx_{ijk}^{n} - zz_{ijk}^{n})\ m(E)}{QF_{ijk}^{010;n-1}\ d} = 0,$$

$$\frac{(wy_{ijk}^{n} - wy_{ijk}^{n-1})\ m(F)}{\tau\ AQF_{ijk}^{n-1}} + \frac{(wy_{ijk}^{n} - zx_{ijk}^{n})\ m(E)}{QF_{ijk}^{001;n-1}\ d} + \frac{(wy_{ijk}^{n} - zz_{i-1,j,k}^{n})\ m(E)}{QF_{ijk}^{-100;n-1}\ d}$$
$$+ \frac{(wy_{ijk}^{n} - zx_{i,j,k-1}^{n})\ m(E)}{QF_{ijk}^{00-1;n-1}\ d} + \frac{(wy_{ijk}^{n} - zz_{ijk}^{n})\ m(E)}{QF_{ijk}^{100;n-1}\ d} = 0,$$

$$\frac{(wz^n_{ijk} - wz^{n-1}_{ijk})\ m(F)}{\tau\ AQF^{n-1}_{ijk}} + \frac{(wz^n_{ijk} - zx^n_{ijk})\ m(E)}{QF^{010;n-1}_{ijk}\ d} + \frac{(wz^n_{ijk} - zy^n_{i-1,j,k})\ m(E)}{QF^{-100;n-1}_{ijk}\ d}$$
$$+ \frac{(wz^n_{ijk} - zx^n_{ijk})\ m(E)}{QF^{0-10;n-1}_{ijk}\ d} + \frac{(wz^n_{ijk} - zy^n_{ijk})\ m(E)}{QF^{100;n-1}_{ijk}\ d} = 0,$$

$$\frac{(zx^n_{ijk} - zx^{n-1}_{ijk})\ m(F)}{\tau\ AQE^{n-1}_{ijk}} + \frac{(zx^n_{ijk} - wy^n_{i,j,k+1})\ m(E)}{QE^{001;n-1}_{ijk}\ d} + \frac{(zx^n_{ijk} - wz^n_{ijk})\ m(E)}{QE^{0-10;n-1}_{ijk}\ d}$$
$$+ \frac{(zx^n_{ijk} - wy^n_{ijk})\ m(E)}{QE^{00-1;n-1}_{ijk}\ d} + \frac{(zx^n_{ijk} - wz^n_{i,j+1,k})\ m(E)}{QE^{010;n-1}_{ijk}\ d} = 0,$$

$$\frac{(zy^n_{ijk} - zy^{n-1}_{ijk})\ m(F)}{\tau\ AQE^{n-1}_{ijk}} + \frac{(zy^n_{ijk} - wx^n_{i,j,k+1})\ m(E)}{QE^{001;n-1}_{ijk}\ d} + \frac{(zy^n_{ijk} - wz^n_{ijk})\ m(E)}{QE^{-100;n-1}_{ijk}\ d}$$
$$+ \frac{(zy^n_{ijk} - wx^n_{ijk})\ m(E)}{QE^{00-1;n-1}_{ijk}\ d} + \frac{(zy^n_{ijk} - wz^n_{i+1,j,k})\ m(E)}{QE^{100;n-1}_{ijk}\ d} = 0,$$

$$\frac{(zz^n_{ijk} - zz^{n-1}_{ijk})\ m(F)}{\tau\ AQE^{n-1}_{ijk}} + \frac{(zz^n_{ijk} - wx^n_{i,j,k+1})\ m(E)}{QE^{010;n-1}_{ijk}\ d} + \frac{(zz^n_{ijk} - wy^n_{ijk})\ m(E)}{QE^{-100;n-1}_{ijk}\ d}$$
$$+ \frac{(zz^n_{ijk} - wx^n_{ijk})\ m(E)}{QE^{0-10;n-1}_{ijk}\ d} + \frac{(zz^n_{ijk} - wy^n_{i+1,j,k})\ m(E)}{QE^{100;n-1}_{ijk}\ d} = 0. \tag{10}$$

3 Numerical experiments

In this section we will present the results obtained by the above mentioned schemes.

Example 1 In this example the exact solution is given by

$$u(x,y,z,t) = \min\left\{\frac{1}{2}\left(x^2+y^2+z^2-1\right)+2t; 0\right\}.$$

The numerical results obtained by using "Hermeline" scheme are plotted in Figures 9 and 10. In the Table 1 we present the results obtained by this scheme.

The numerical results obtained by using "Coudiére–Hubert" scheme are plotted in Figures 11 and 12. In the Table 2 we present the results obtained by this scheme.

In both cases we set $\tau = h^2$, $z = 0.00390625$, $N_1 = N_2 = N_3 = 40$.

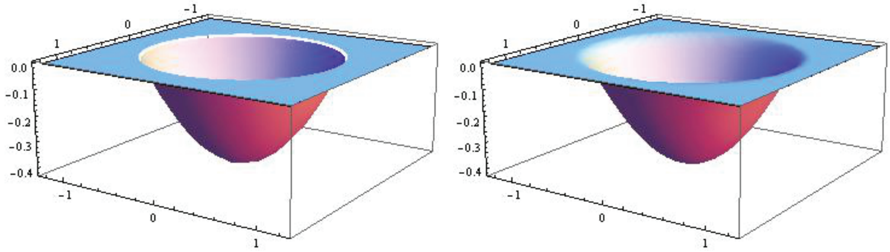

Figure 9: Exact (left) and numerical (right) solution after 10 time steps using "Hermeline" scheme, $N_1 = N_2 = N_3 = 40$

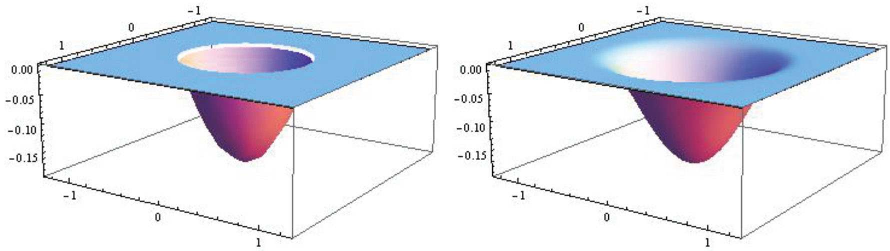

Figure 10: Exact (left) and numerical (right) solution after 40 time steps using "Hermeline" scheme, $N_1 = N_2 = N_3 = 40$

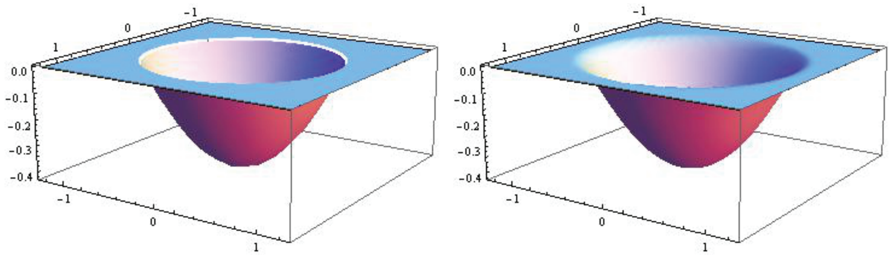

Figure 11: Exact (left) and numerical (right) solution after 10 time steps using "Coudiére–Hubert" scheme, $N_1 = N_2 = N_3 = 40$

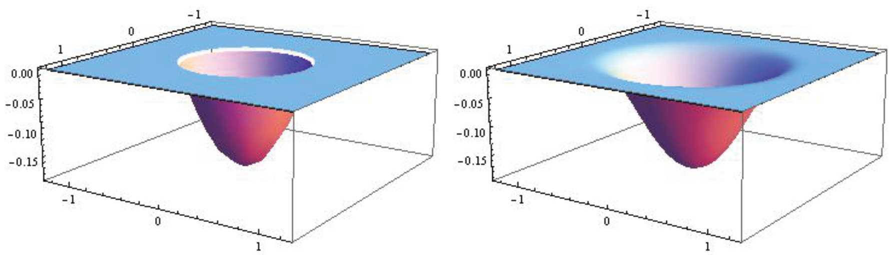

Figure 12: Exact (left) and numerical (right) solution after 40 time steps using "Coudiére–Hubert" scheme, $N_1 = N_2 = N_3 = 40$

N	L_2 error	EOC L_2 error	L_2 gradient error	EOC L_2 gradient error
10	6.9985e-2	–	2.7369e-1	–
20	3.7869e-2	0.9084	2.2711e-1	0.2691
40	1.9153e-2	0.9611	1.7367e-1	0.3871
80	9.7404e-3	0.9755	1.3319e-1	0.3829

Table 1: EOC and errors obtained by DDFV "Hermeline" scheme

N	L_2 error	EOC L_2 error	L_2 gradient error	EOC L_2 gradient error
10	6.5323e-2	–	2.6010e-1	–
20	3.4497e-2	0.9435	2.1560e-1	0.2707
40	1.7832e-2	0.9507	1.7224e-1	0.3239
80	1.0902e-2	0.7097	1.3932e-1	0.3060

Table 2: EOC and errors obtained by DDFV "Coudiére–Hubert" scheme

4 Conclusion

In this work we have compared two new schemes for solving curvature driven level set equation in 3D based on dual volumes. Concerning the numerical experiment we can say, that our expectations were fulfilled by obtaining EOC of the L_2 error tending to 1 in both cases. Because of the non-smooth function of the exact solution better results could not have been expected. Concerning EOC of the L_2 gradient error, it is tending to be $\frac{1}{3}$, what was also expected. Coudiére–Hubert scheme has some advantages, the biggest one will appear thanks to the expression of the gradients in proving stability and convergence of the given scheme.

References

[1] Andreianov, B., Bendahmare, M., Karlsen, K. H.: *A Gradient Reconstruction Formula for Finite Volume Schemes and Discrete Duality.* In: Finite Volume For Complex Applications, Problems And Perspectives. 5th International Conference, *Wiley*, London, 2008, 161–168.

[2] Andreianov, B., Boyer, F., Hubert, F.: *Discrete duality finite volume schemes for Leray–Lions type elliptic problems on general 2D meshes.* Numerical Methods PDE **23**, 1 (2007), 145–195.

[3] Coudiére, Y., Hubert, F.: *A 3D discrete duality finite volume method for nonlinear elliptic equations.* Algoritmy **2009** (2009), 51–60.

[4] Evans, L. C., Spruck, J.: *Motion of the level sets by mean curvature I.* J. Differential Geometry **3** (1991), 635–681.

[5] Eymard, R., Gallouë, T., Herbin, R.: *Finite volume methods.* Handbook of Numerical Analysis (Ph. Ciarlet, J. L. Lions, eds.), **3** (2000), 713–1018.

[6] Handlovičová, A., Kotorová, D.: *Stability of the semi-implicit discrete duality finite volume scheme for the curvature driven level set equation in 2D.* Tatra Mountains Mathematical Publications, accepted.

[7] Hermeline, F.: *A finite volume method for approximating 3D diffusion operators on general meshes*. Journal of Computational Physics **228**, 16 (2009), 5763–5786.

[8] Kotorová, D.: *Discrete duality finite volume scheme for the curvature-driven level set equation*. Acta Polytechnica Hungarica **8**, 3 (2011), 7–12.

[9] Kotorová, D.: *Discrete duality finite volume scheme for the curvature driven level set equation in 3D*. In: Advances in architectural, civil and environmental engineering [electronic source]: 22nd Annual PhD Student Conference, *Nakl. STU*, Bratislava, 2012, 33–39.

[10] Kotorová, D.: *3D numerical schemes for the level set equation based on discrete duality finite volumes*. to appear.

[11] Sethian, J. A.: Level Set Methods and Fast Marching Methods: Evolving Interfaces in Computational Geometry, Fluid Mechanics, Computer Vision, and Material Science. *Cambridge University Press*, New York, 1999.